# Multichannel recordings from membranes which contain gap junctions

K. Manivannan, S. V. Ramanan, R. T. Mathias, and P. R. Brink
Department of Physiology and Biophysics, State University of New York, Stony Brook, New York 11794-8661

ABSTRACT We have studied multichannel patch-clamp recordings in earthworm axon septal membranes that contain gap junctions. Though all channels have the same conductance and selectivity, the probabilities of the conductance levels in the majority of the recordings could not be fit by assuming independent and identical channels; in these cases, we found that at least two different open probabilities were required to explain the data. The data thus suggest that, within one junctional membrane complex, there exists a heterogenous channel population of similar but not identical channel types. The analysis also revealed cases where cooperativity between individual channels was the only explanation for the amplitude histograms of the observed multichannel activity. The conclusions drawn are based on a theoretical analysis of multichannel current-amplitude histograms. We derive two tests for independent and identical channels. We analyze the effects of mode shifting. These results are based on the ratio of peaks in the histograms; they are independent of the number of channels in the patch and the model of channel gating. In some cases failure to fulfill the criteria of these tests implied an interdependence or cooperativity between channels. Lastly, we have devised statistical tests for stability of the recording in the presence of variance due to finite sample size.

## INTRODUCTION

Patch-clamp recordings from a single ionic channel have proved to be an effective way of extracting information about the conformational states of gating macromolecules. The theory of continuous-time Markov chains (Cox and Miller, 1965; Colquhoun and Hawkes, 1981; Fredkin et al., 1985) is most often used as the basis for channel analysis. Such analysis of these recordings can provide information about the number of conformational states and the transition rates between them.

In our studies, patches containing only one channel constitute a minority of recordings. In most cases, more than one channel is found to be functioning within a patch. In the case of gap junctions, moreover, such a scenario is expected to be a common one. Anatomical studies, mostly freeze fracture, have revealed that individual gap junction channels tend to aggregate in groups. The number of channels in these groups is highly variable. Liver cell gap-junction plaques (Goodenough, 1975) are classic examples of cases where hundreds or thousands of channels are found to be aggregated together and the channel density is of the order of $1{,}000/\mu m^2$. These structures can cover several square micrometers and, because many such plaques exist, can account for as much as 10% of the membrane surface area of a liver cell. There are many other examples of gap-junction plaques that contain tens to hundreds of individual channels where the channel density is in the range of $10–100/\mu m^2$. The gap junctions of the earthworm septal membranes form aggregates with typically 10–100 channels, or particles, found in close association (Kensler et al., 1979). The same is true for frog cardiac myocytes (Kensler et al., 1977). Recording the activity of multiple channels in a patch, even if most of the channels in a cluster rarely open (see e.g., Tuttle et al., 1986), is probable given such morphological constraints. Multichannel analysis is a necessary step, therefore, in understanding the gating behavior of these membrane channels.

The construction of an amplitude histogram of the distribution of current is a first step in interpreting multichannel recordings. Provided the signal-to-noise ratio is sufficiently high (Sachs et al., 1982), it is possible to discern Gaussian distributions in the histogram at current levels corresponding to various numbers of channels simultaneously open. The shapes of these peaks may be distorted from the expected Gaussian because of the limited bandwidth of the system; however, corrections for this are possible (Colquhoun and Sigworth, 1983).

Analysis of amplitude histograms from multichannel recordings generally has been made in the context of an assumption of identical and independent channels in a patch. For channels with the same conductivity and selectivity, the assumption that the gating properties are identical is a natural one; but it is entirely possible that channels of the same type need not adhere to this assumption. We find channels with identical conduc-

Address correspondence to Dr. Brink.


0006-3495/92/01/216/12 $2.00

tances and selectivities but differing open probabilities. We refer to these as "similar" channels. Similarity could result from channel-channel interaction, which alters open time, or from protein subunits of channels that are functionally different or in different conformational states as a result of ligand binding, for example.

The channel of interest in this regard is the 100-pS channel found in the septal membrane of earthworm (Brink and Fan, 1989). The initial analysis of the amplitude histograms revealed that the occupancy probabilities for 60% of the recordings could not be fit assuming independent and identical channels. This result prompted us to evaluate the recordings to establish that the multichannel recordings contained channels with the same conductance and selectivity, thus being at least "similar" channels. We attempted to distinguish among the following cases: (1) independent and identical channels; (2) independent and similar channels; (3) nonindependent and similar channels.

We discuss these possibilities in terms of channel behavior in general as well as with regard to the potential role of such behaviors for gap junctions relative to their function in tissues.

## THEORY

# Fits for amplitude histograms

### Case 1: Independent and identical channels

Korn et al. (1981) and Colquhoun and Sigworth (1983) have described fitting of amplitude histograms to binomial distributions. We give the relevant results.

The amplitude histogram is an estimate of $f(i)\Delta i = P(i \le I \le i + \Delta i)$, where f($i$) is the probability density function for $I$ and $P(.)$ indicates the "probability of" the event in parentheses. Assume that we have $M$ channels in the patch, each of which has the property

$$I_{1,n} = \begin{cases} i_1 \text{ with probability } p_1 \\ 0 \text{ with probability } (1 - p_1), \end{cases}$$

where $I_{1,n}$ is the change in current produced by the opening and closing of the $n$th channel. The background thermal noise $I_b(t)$ should be normally distributed, so we assume the probability density function for $I_b$ to be

$$f_b(i, \sigma_b^2) = \frac{1}{\sigma_b\sqrt{2\pi}} e^{-i^2/2\sigma_b^2}$$

The total current is

$$I(t) = I_b(t) + \sum_{n=1}^{M} I_{1,n}(t)$$

and the probability density function is computed by convolving $f_b(i) \otimes [f_{i_1}(i)]^M$ where $[\ ]^M$ indicates an $M$th-order convolution. The result is

$$f_I(M) = \sum_{n=0}^{M} B(M, n, p_1) f_b(I - ni_1, \sigma_b^2) \qquad (1)$$

where

$$B(M, n, p_1) = \frac{M!}{n!(M-n)!} p_1^n (1 - p_1)^{N-n}. \qquad (2)$$

Frequently, the open channel does add excess noise, due, for example, to shot noise (Sigworth, 1985), finite ion passage times (Stevens, 1972), and thermal fluctuations of channel structure (Läuger, 1983). An additional source of noise is the presence of substates close to the major conducting level; such substates are found in the channel being studied. These substates may also cause the current flowing when $n$ channels are simultaneously open to differ substantially from $n$ times the unitary current $i_1$, provided the channels have different open probabilities as well as different substate occupancy probabilities (Ramanan and Brink, manuscript in preparation). Moreover, if the substates are clustered close to the unitary peak, they should merely broaden the main peaks and not obscure them. We denote, then, the current passed by $n$ simultaneously open channels by $I_n$ and the variance of the background thermal noise by $\sigma_b^2$, and assume that the excess noise due to the open channel is Gaussian with variance $\sigma_o^2$. The $M$-channel histogram for this situation is

$$f_I(M) = \sum_{n=0}^{M} B(M, n, p_1) f_b(I - I_n, \sigma_b^2 + n\sigma_o^2) \qquad (3)$$

### Two tests for independent and identical channels

An actual experiment requires that we estimate the density function from a finite set of data points; consequently, we may miss one or more of the higher order and less probable peaks. We provide two checks to verify that a histogram is consistent with the binomial density function (Eq. 3) generated by independent and identical channels. Both of the tests may be performed without knowledge of the number $N$ of channels in the patch.

(*Test 1*) Let $P_0$ denote the probability of having no channels open and $P_m$ the probability of $m$ channels being open. These probabilities can be estimated from the area under the associated peak in a normalized amplitude histogram. For identical and independent channels with open probability $p$, these probabilities are given by $P_m = B(N, m, p)$. From Eq. 2, it follows that the parameter

$$\Delta \equiv \frac{P_1^2}{P_0 P_2} = \frac{2N}{N-1}. \qquad (4)$$

$\Delta$ is seen to decrease monotonically from 4 to 2 as $N$ is varied from 2 to $\infty$:

$$2 \le \Delta < 4. \qquad (5)$$

(*Test 2*) We derive an upper bound for $P_m$ when $m$ is an interior level, i.e., $m \neq 0$ and $m$ is not the most conductive level. For fixed $N$ and $m$, we can differentiate Eq. 2 with respect to $p$ to show that the $m$th occupation probability $P_m = B(N, m, p)$ is maximum when $p = m/N$. For this value of $p$, we find

$$B_{max}(N, m) \equiv B\left(N, m, \frac{m}{N}\right) = \frac{N!}{m!(N-m)!} \left(\frac{m}{N}\right)^m \left(1 - \frac{m}{N}\right)^{N-m}.$$

It follows that

$$\frac{B_{max}(N+1, m)}{B_{max}(N, m)} = \frac{[1 + 1/(N-m)]^{N-m}}{(1 + 1/N)^N}.$$

Since $(1 + 1/m)^m$ is a monotonically increasing function of $m$, we find for $m$ corresponding to an interior level that

$$P_m \leq B_{max}(m + 1, m) = \left(\frac{m}{m + 1}\right)^m. \quad (6)$$

For instance, $P_1$ can never be greater than ½, $P_2$ can never be greater than 4/9, and so on.

### Case 2: Independent and similar channels with two open probabilities

As stated in the introduction, we record data where the amplitude histogram cannot be fitted by the assumption by functions of the form above, i.e., the channels are not independent and identical. To analyze this possibility, we need to derive the density function for a patch containing more than one type of channel. In what follows, we provide an expression for the current distribution for a patch containing two types of channels, each with its own associated open probability.

Assume that there are $N$ total channels in the patch. Of these, $N - M$ channels have the property stated above; the remaining $M$ channels have the identical properties, except that their open probability is $p_2$. A calculation identical to the one done above shows that the current histogram is described by

$$f_I(N) = \sum_{n=0}^{N}\left[\sum_{k=0}^{n} B(N - M, k, p_1)B(M, n - k, p_2)\right] \times f_b(I - I_n, \sigma_b^2 + n\sigma_o^2). \quad (7)$$

### Case 3: Cooperativity in two-channel histograms

More detailed calculations can be performed in cases where the number of channels $N$ is small. Here we provide a few particular results for the case of two channels. In this case, with the two channels having open probabilities $p_1$ and $p_2$, the coefficients $P_m$ are given by

$$P_0 = (1 - p_1)(1 - p_2), P_2 = p_1p_2; \quad P_1 = p_1(1 - p_2) + p_2(1 - p_1) \quad (8)$$

and $\Delta$ as defined in Eq. 4 obeys the inequality

$$\Delta \geq 4. \quad (9)$$

Equality implies that the two channels have the same open probability. If $\Delta < 4$, solving Eq. 8 for $p_1$ and $p_2$ will yield complex values. Therefore, a two-channel amplitude histogram with $\Delta < 4$ cannot be fit by two independent channels, even if they have different probabilities. We will describe the condition

$$\Delta < 4 \quad (10)$$

for two channels as the condition characterizing *cooperative* behavior.

### Mode shifting cannot make two independent channels appear cooperative

Single-channel behavior is often characterized by "mode shifting" (Hess et al., 1984). This term describes a situation where the channel enters a subset of conformations where the probability of opening may be quite different from that observed in the normal "mode" of operation. The observed open probability of the channel may then vary across different segments of the record. For two channels, this effect can be modeled by assuming that the channels have time-dependent probabilities $p_1(t)$ and $p_2(t)$. However, such time dependence of the probabilities cannot lead to an apparent overall cooperative behavior as defined by Eq. 10, provided that the channels are independent. For:

$$\begin{aligned} P_1^2 &= (1 - P_0 - P_2)^2 = 4P_0P_2 + (1 - P_0 + P_2)^2 - 4P_2 \\ &= 4P_0P_2 + (\overline{p_1} + \overline{p_2})^2 - 4\overline{p_1p_2} \quad \text{(using Eq. 8)} \\ &= 4P_0P_2 + (\overline{p_1} - \overline{p_2})^2 - 4(\overline{p_1}\,\overline{p_2} - \overline{p_1}\,\overline{p_2}) \end{aligned}$$

Here $\overline{p_1}$, for instance, denotes the mean of $p_1$ over the time of observation. If the channels are independent, then we must have

$$\overline{p_1}\,\overline{p_2} = \overline{p_1}\,\overline{p_2}, \quad (11)$$

and therefore $P_1^2 \geq 4P_0P_2$, i.e., $\Delta \geq 4$, which is the criterion for independent channels (see Eq. 9).

In the above discussion, we have treated the probabilities as if they are instantaneously measurable. For channel data, the occupation probabilities are found by calculating the total time of a number of sojourns at a particular conductance level. In practice, then, inequality (Eq. 4) would imply cooperativity only if it were found in a record which was statistically "long enough" (see stability section below for related discussion).

## Stability of a recording

The level occupation probabilities can vary from segment to segment in a record because of the probabilistic nature of the process. We derive a bound on these fluctuations for the simple model.

$$C \underset{\beta}{\overset{\alpha}{\rightleftharpoons}} O. \quad (12)$$

Then $\alpha \exp(-\alpha t)$ is the probability density function (pdf) for openings of length $t$ and $\beta \exp(-\beta t)$ is the similar pdf for closures. For a time $T$ of single-channel recording, there are two distributions of interest.

### Distribution of the number of episodes in time $T$ of recording

The probability that there are exactly $r$ openings and $r$ closures, the combined duration of which is equal to $T$, is $[(f_o)^r \otimes (f_c)^r](T)$, where $(\,)^r$ is an $r$th-order convolution. The normalized distribution $H(r, T)$ of the number of openings in time $T$ is

$$H(r, T) = \frac{\dfrac{1}{(r-1)!}\left[\dfrac{\alpha\beta T}{(\alpha - \beta)}\right]^r I_{r-1/2}\left(\dfrac{\alpha - \beta}{2}T\right)}{\dfrac{2(\alpha^2 - \beta^2)}{\alpha\beta}\sqrt{\dfrac{\pi}{(\alpha - \beta)T}}} \sinh(u) \quad (13)$$

where $u = (\alpha + \beta)T/2$ and $I$ is a modified Bessel function, as defined in Abramowitz and Stegun (1970, p. 374). The mean $\bar{r}$ of this distribution is the average number of openings (or closures) in the time $T$. This is given by

$$\bar{r} = \frac{\alpha^2 + \beta^2}{(\alpha + \beta)^2} + \frac{\alpha\beta T}{\alpha + \beta}\frac{1}{\tanh(u)} \quad (14)$$

The associated variance $\sigma_r^2$ is given by

$$\sigma_r^2 = -\frac{2\alpha\beta(\alpha-\beta)^2}{(\alpha+\beta)^4} - \frac{\alpha^2\beta^2T^2}{(\alpha+\beta)^2\sinh^2(u)} + \frac{\alpha\beta T(\alpha^2+\beta^2)}{(\alpha+\beta)^3\tanh(u)} \quad (15)$$

In the limit that $\alpha\beta T/(\alpha+\beta) \gg 1$, it follows that $u \gg 1$, and we can write

$$\bar{r} \sim \frac{\alpha\beta T}{\alpha+\beta}; \quad \sigma_r^2 \sim \frac{\alpha\beta T(\alpha^2+\beta^2)}{(\alpha+\beta)^3} = \bar{r}\frac{(\alpha^2+\beta^2)}{(\alpha+\beta)^2} < \bar{r} \quad (16)$$

Thus the distribution for $r$ follows Poisson-like statistics.

### Distribution of the open probability in time *T* of recording

Assume that there are exactly $\bar{r}$ openings (and closures) in time $T$, where $\bar{r}$ is the mean number of openings in time $T$, as given by Eq. 14. The distribution of the open probability $p$ is given by $[(f_c)^{\bar{r}}\,(qT)]\,[(f_o)^{\bar{r}}\,(pT)]$. Here $q = 1 - p$ and $(\,)^r$ is an $r$th-order convolution. The normalized distribution $G(p, T)$ that we find an open probability of $p$ in time $T$ is

$$G(p,t) = \frac{\dfrac{p^{\bar{r}-1}}{(\bar{r}-1)!}\dfrac{q^{\bar{r}-1}}{(\bar{r}-1)!}\exp(-\alpha pT)\exp(-\beta qT)}{\dfrac{\sqrt{\pi}}{(\bar{r}-1)!}[(\alpha-\beta)T]^{1/2-\bar{r}}\exp[-(\sigma+\beta)T]I_{\bar{r}-1/2}[(\alpha-\beta)T/2]}\,dp$$

The mean $\bar{p}$ and variance $\sigma_p^2$ of this distribution are given by

$$\bar{p} = \tfrac{1}{2} - I_{\bar{r}+1/2}(z)/I_{\bar{r}-1/2}(z)$$

and

$$4\sigma_p^2 = I_{\bar{r}+3/2}(z) + 2\frac{I_{\bar{r}+1/2}(z)}{(\alpha-\beta)T} - \frac{[I_{\bar{r}+1/2}(z)]^2}{I_{\bar{r}-1/2}(z)},$$

where $z = (\alpha - \beta)T/2$. In the limit when $\alpha\beta T/(\alpha+\beta) \gg 1$, $\bar{r}$ is large, and the above expressions asymptotically (Abramowitz and Stegun, 1970, p. 378, Eqs. 9.7.8 and 9.7.9) become

$$\bar{p} \sim \frac{\alpha}{(\alpha+\beta)} \quad \text{and} \quad \sigma_p^2 \sim \frac{\overline{pq}}{2\bar{r}}. \quad (17)$$

Because of the $\sim\bar{r}$ variance in $\bar{r}$ demonstrated earlier (see Eq. 16), a better estimate for the lower bound for $\sigma_p^2$ may be found by replacing $\bar{r}$ by $\bar{r} + \sqrt{\bar{r}}$ in the above expression.

The results above are for the simple model Eq. 12. The presence of additional closed or open states and autocorrelations of finite duration in more complex models can only cause the fluctuations to increase in magnitude. Here we have arbitrarily chosen $5\sigma_p$ as a bound on the actual standard deviation for $\bar{p}$. Recordings of single channels have shown (Brink, unpublished observations) that the mean closed time is in the range 20–150 ms. We have set $\beta$ at 100 ms in the calculation of the estimates for the fluctuations in the probability $p$.

Given the variance $\sigma_p^2$ expected in a time $T$ for a single channel, we can easily calculate the variances for any collection of channels. For example, consider an assortment of $M$ identical channels described by Eq. 12. The level where $n$ of these channels are open has a mean occupation probability $B(M, n, \bar{p})$. The upper and lower bounds for this probability are given by $B(M, n, \bar{p} + 5\sigma_p)$ and $B(M, n, \bar{p} - 5\sigma_p)$.

## METHODS

## Preparation of membranes containing gap junctions

The methods used to record multichannel data directly from gap junction–containing membranes are those demonstrated by Brink and Fan (1989). All patch recordings were performed with identical solutions in the bath and pipette. The solution consisted of 135 or 170 mM CsCl, 30 mM tetraethylammonium (TEA) Cl, 0.6 mM EGTA, 0.1 mM $CaCl_2$, 10 mM Hepes, 1 mM $CoCl_2$ and 1 mM $NiCl_2$. In some experiments 2 mM $ZnCl_2$ was also present. The pH of the solution was 7.0, and HCl was used to adjust the pH initially. In one experiment illustrated in the results section, the bathing medium started out with 170 mM CsCl but was exchanged with one containing 340 mM CsCl.

## Processing

Data are acquired on videotape through an interface device (DR-384, Neuro Data Instruments Corp., New York, NY), the combined system having an effective bandwidth of 20 kHz. During playback to the analog-digital (A/D) converter, the data are filtered by a 9-pole Bessel filter with 3-dB low-pass frequency which is continuously variable from 100 Hz to 30 kHz (model LPF-30, World Precision Instruments, Sarasota, (FL). The entire system, including the patch clamp, is experimentally calibrated for dead time ($T_d$) at various frequencies by injecting a square current at the patch-clamp headstage input and finding the input pulse duration at which the maximum of the output signal attenuates to half that of the input amplitude. The data presented here were collected with the low-pass filter set at 500 Hz throughout, corresponding to a dead time of 360 μs.

The sampling rate of the A/D converter (model DT-2801A, Data Translation, Marlborough, MA) is set at a rate equal to or less than half the dead time corresponding to the low-pass filter frequency. Due to the limitations caused by the microprocessor's (80xxx) segmenting of memory, at most 32,767 samples may be acquired continuously before the A/D output must be directed to a different segment. As the data from one segment is saved to a high-speed virtual memory while the A/D is storing on another segment, at most 500 μs of data is lost between adjacent data files, where each file corresponds to a time equal to (no. of samples) × (sample period). All the data collected were digitized at 180 μs.

The data are digitized into 4,096 bins corresponding to the 12-bit resolution of the A/D converter. A raw histogram of frequency of occurrence in various bins is then computed. Discriminators between the various currents corresponding to all channels closed, one channel open, two channels open, and so on are set with reference to the amplitude histogram. Probabilities of the various conducting states are then readily extracted.

Fits to the amplitude histograms are done as described in the theory section. All programs were written in QuickBasic on an IBM PC.

## RESULTS

All data shown in this section are derived from excised patches. Typical channel behavior is illustrated in Fig. 1. The holding potential was +87 mV. The sample shown is a 5-s portion of an 8 min record (033189, Table 2). At least two channels are present and, at either open level, substates are observable. The dashed horizontal lines or rulers are drawn to illustrate the substates and the ground state. The rulers were drawn at 0, 6.5, 7.35, 13.0, 13.85, and 14.7 pA. The unitary conductance of the channel shown in this recording was 85 pS with 135 mM CsCl on both sides of the patch. The unitary current was 7.4 pA, whereas the major substate current in the first open level was 6.5 pA. Substates like those shown here, the amplitudes of which are close to either the baseline noise or the open channel current, will cause shifts in the peaks of the amplitude histograms of current distribution.

It should be noted that the substates are long lived and are also a probable cause for the variability of single-channel conductance observed from preparation to preparation. Brink and Fan (1989) first noted that the conductance varied from 90 to 110 pS in 135 mM CsCl. When 170 mM CsCl is used, the conductance varied from preparation to preparation in a similar fashion (120–150 pS). Depending on their frequency of occurrence, the substates can weight the unitary current observed in the amplitude histogram such that the perceived single channel conductance appears variable.

The following examples (Figs. 2–6) will illustrate the three cases previously described: independent and identical channels (case 1, Fig. 2), independent and similar channels (case 2, Figs. 3–5) and nonindependent and similar channels (case 3, Fig. 6).

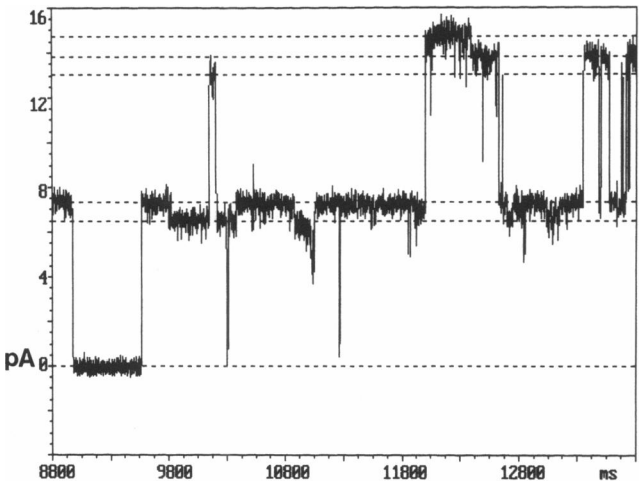


FIGURE 1 Trace of a 5-s record from a detached patch of an 85-pS channel at +87 mV. CsCl concentration was 135 mM. Note that the range of conductances observed for the "100"-pS channel is 80–110 pS (Brink and Fan, 1989). Note the presence of two conducting states for the open channel. There are substates observable at each open state. The dotted lines in the inset are rulers set at 0, 6.5, 7.35, 13.0, 13.85, and 14.7 pA.

## Case 1: Independent and identical channels

Fig. 2 shows the analysis of an 8 min sample (033089 B in Tables 1 and 2) from an excised patch at a holding potential of +77 mV. The maximum number of channels seen open during the 8 min was four. This data set is displayed as an example of independent and identical channels. All three histograms of Fig. 2 were fit assuming independent and identical channels. Fig. 2, *A* and *B*, shows the amplitude histogram from the first and the second halves (4.3 min each); Fig. 2 *C* is the composite of the entire 8 min. Note that *A* and *B* are visually similar, an indication that the recording was stable throughout the full 8 min. To establish whether or not the recording was stable for the whole time period, the following test was performed. The level occupation probabilities (calculated areas under the peaks) were determined for the two halves shown and are listed in Table 1. Table 1 also shows the allowed standard deviations of the occupation probabilities estimated using Eq. 17. The variation of the probabilities from the first to the second half are seen to be within the tolerances.

Table 1 also shows the composite level occupation probabilities, which are consistent with the first test (Eq. 5) for independent identical channels, with the parameter $\Delta$ obeying $2 \leq \Delta = 2.5 \leq 4$. The level probabilities are also consistent with the second test given by Eq. 6.

The fits (*dotted lines*) shown in *A* and *B* are made using the same parameters as the fit for the composite histogram *C*. The inset in *C* is an enlargement of the composite histogram for currents corresponding to three

FIGURE 2 (*A* and *B*) Amplitude histograms of the first and second halves of an 8 min recording of a 97-pS (averaged over substates) channel at +77 mV. (*C*) Composite histogram for the entire 8.6 min. The inset shows an enlargement of the smaller peaks. The dotted line in *C* is the fit made using Eq. 3 in the text for identical and independent channels. The dotted lines in *A* and *B* are made using the same parameters as in *C*. Five channels, all with an open probability of 0.19, are used. The variances used are $\sigma_b = 0.38$ pA and $\sigma_0 = 0.8$ pA for the thermal noise and excess open channel noise, respectively. The currents for the different levels (see Eq. 3 of text) are $I_1 = 7.43$ pA, $I_2 = 13.75$ pA, $I_3 = 18.60$ pA, $I_4 = 23.2$ pA, and $I_5 = 27.6$ pA. The solution on both sides of the membrane contained 135 mM of CsCl. The y-axis is the number of digitized points.

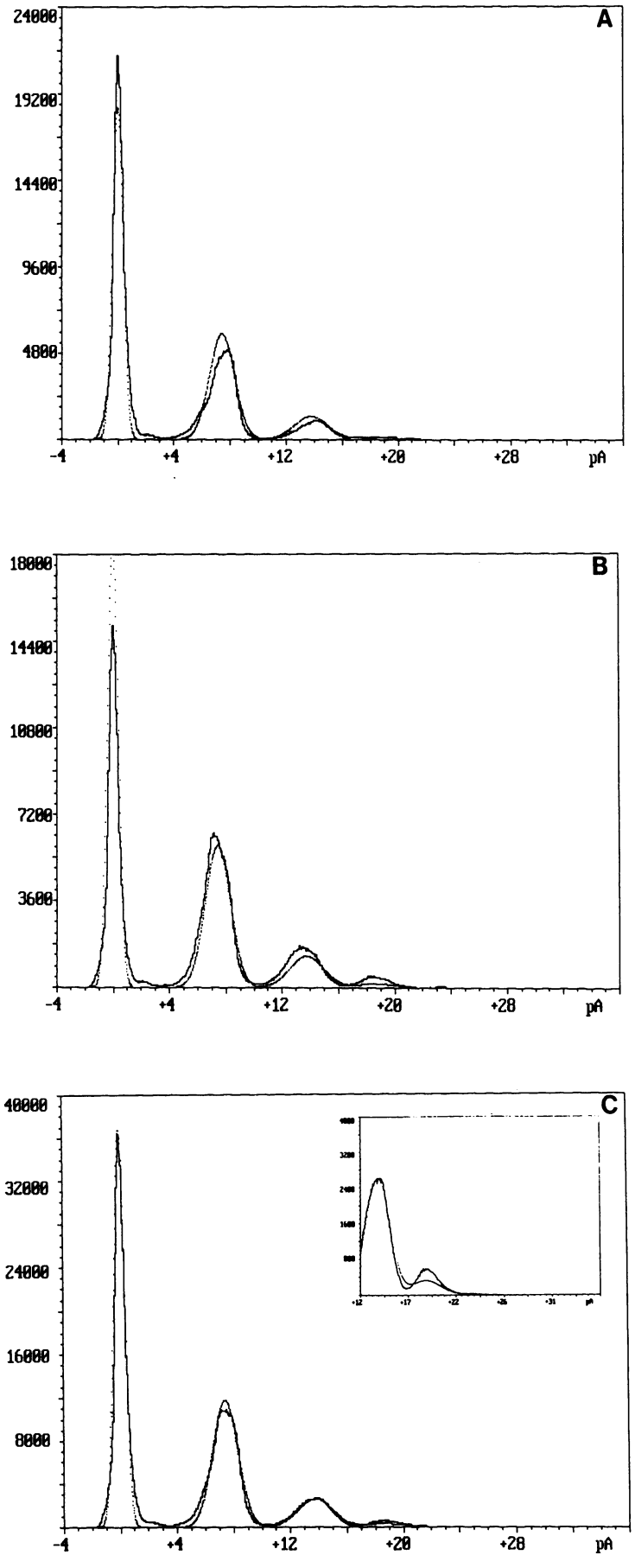
A
24000
19200
14400
9600
4800
-4
+4
+12
+20
+28
pA
B
18000
14400
10800
7200
3600
-4
+4
+12
+20
+28
pA
C
40000
32000
24000
16000
8000
-4
+4
+12
+20
+28
pA

**TABLE 1 Stability of multichannel records**

| | $P_0$ | $P_1$ | $P_2$ | $P_3$ | $P_4$ | $P_5$ | $P_6$ | $P_7$ | $P_8$ | $P_9$ |
|---|---|---|---|---|---|---|---|---|---|---|
| 033089 B | | | | | | | | | | |
| Composite | 49.0 | 37.4 | 11.3 | 2.3 | 0.1 | — | — | — | — | — |
| LOP fit | 43.1 | 40.4 | 14.2 | 2.2 | 0.1 | — | — | — | — | — |
| Variance | 13.9 | 4.4 | 7.3 | 2.1 | 0.1 | — | — | — | — | — |
| 1st half | 57.2 | 33.1 | 8.5 | 1.2 | 0.04 | — | — | — | — | — |
| 2nd half | 40.7 | 41.6 | 14.0 | 3.4 | 0.2 | — | — | — | — | — |
| 033089 A | | | | | | | | | | |
| Composite | 0.9 | 9.6 | 21.3 | 26.3 | 23.7 | 12.6 | 4.5 | 0.9 | 0.2 | 0.009 |
| LOP fit | 0.7 | 6.9 | 19.8 | 28.7 | 24.6 | 13.4 | 4.7 | 1.0 | 0.1 | 0.007 |
| Variance | 0.6 | 4.5 | 7.5 | 3.8 | 3.8 | 5.7 | 3.3 | 1.0 | 0.2 | 0.007 |
| 1st half | 0.7 | 9.5 | 23.2 | 29.3 | 24.3 | 10.1 | 2.9 | 0.1 | 0.1 | 0.007 |
| 2nd half | 1.3 | 9.8 | 19.1 | 23.1 | 23.0 | 15.4 | 6.3 | 1.7 | 0.2 | 0.013 |
| 071890 | | | | | | | | | | |
| Composite | 0.4 | 46.2 | 53.5 | — | — | — | — | — | — | — |
| LOP fit | 0.4 | 46.2 | 53.5 | — | — | — | — | — | — | — |
| Variance | 0.3 | 5.6 | 5.2 | — | — | — | — | — | — | — |
| 1st half | 0.7 | 41.7 | 57.6 | — | — | — | — | — | — | — |
| 2nd half | 0.07 | 50.6 | 49.4 | — | — | — | — | — | — | — |

LOP, Level occupation probability (Eqs. 3 and 7).

**TABLE 2 Probabilities in multichannel records**

| File | $V_H$ *mV* | $T$ *min* | $N$ | $\Delta$ | $n_1$ | $p_1$ | $n_2$ | $p_2$ |
|---|---|---|---|---|---|---|---|---|
| 101988 | +60 | 4 | 3 | 580 | 2 | 0.03 | 1 | 0.96 |
| 012789 | +84 | 9 | 4 | 2.4 | 2 | 0.15 | 2 | 0.33 |
| 033089 A | +45 | 8 | 9 | 8.1 | 8 | 0.31 | 1 | 0.87 |
| | −55 | 4.3 | 6 | 0.8 | 6 | 0.38 | — | — |
| | +65 | 18 | 6 | 3.8 | 6 | 0.24 | — | — |
| | −64 | 4.3 | 4 | 5.3 | 3 | 0.15 | 1 | 0.65 |
| B | +77 | 8 | 4 | 2.5 | 5 | 0.19 | — | — |
| | +90 | 14.5 | 4 | 2.5 | 4 | 0.17 | — | — |
| | +65 | 4.5 | 5 | 4.0 | 5 | 0.22 | — | — |
| 033189 | +87 | 8.5 | 2 | 3.7 | 2 | 0.35 | — | — |
| | −28 | 7 | 2 | 44 | 1 | 0.63 | 1 | 0.98 |
| | +112 | 8 | 3 | 7.0 | 1 | 0.23 | 2 | 0.74 |
| | −48 | 4 | 2 | 14 | 1 | 0.43 | 1 | 0.90 |
| 062790 | +50 | 4 | 6 | 3.3 | 2 | 0.08 | 4 | 0.74 |
| 071890 | +61 | 8 | 2 | 105 | 1 | 0.54 | 1 | 0.99 |
| | +70 | 10 | 2 | 5.4 | 1 | 0.41 | 1 | 0.68 |
| 072490 | +48 | 16 | 3 | 29 | 1 | 0.76 | 2 | 0.96 |
| 072590-1 | +45 | 4.5 | 3 | 9.4 | 1 | 0.29 | 1 | 0.74 |
| 072590-2 | +40 | 8 | 2 | 774 | 1 | 0.03 | 1 | 0.95 |
| 080890 | +50 | 2.3 | 2 | 1.4 | — | — | — | — |

$N$, maximum number of channels seen simultaneously open; $\Delta$ is defined in Eq.4; $n_1$ is the number of channels with probability $p_1$ and $n_2$ is the number of channels with probability $p_2$ needed to fit the amplitude histogram.

and four openings. The parameters for the fit are given in the legend.

We note that the fit for Fig. 2 is made assuming that there are five independent and identical channels in the patch, which is one more than the maximum number of channels observed during the 8 min of the record. It is possible that using a higher number of channels may yield a better fit, and procedures to evaluate the actual number of channels according to maximum likelihood have been noted in the literature (Korn et al., 1981). As we are primarily interested in finding whether a fit using independent and identical channels is consistent with the data, we have not applied sophisticated tests to estimate the number of channels in the patch. Instead, we have increased this number in steps of one and stopped the process of fitting as soon as the fit is satisfactory.

## Case 2: Independent and similar channels

The data shown in Fig. 2 were from a patch that lasted 1.8 h, and the recordings analyzed in Fig. 2 represent activity 55 min after the formation of the patch. Fig. 3 shows 8 min of data taken from the same excised patch almost immediately after it was excised. It is an illustration of the second case: independent and similar channels.

Fig. 3 presents the data for experiment 033089 A in Tables 1 and 2, from the excised patch at a potential of +45 mV. A maximum of nine channels was observed to be active during the 8 min. The recording is from the same patch as that depicted in Fig. 2, where the maximum observed number of channels was four rather than nine. Clearly run-down occurred over the 55-min interval between experiments. Table 1 shows the stability analysis applied to the nine-channel recording of 033089 A. The level occupation probabilities are within the variance predicted by Eq. 17. In addition, the composite occupation probabilities shown in Table 1 for 033089 A do not violate the consistency conditions for independent and identical channels given in Eq. 6, but the parameter Δ (defined in Eq. 4) is equal to 8.1, which, according to Eq. 5, indicates that there are channels with different characteristic probabilities in the patch. Indeed, the composite histogram can be fitted by assuming that there are eight channels, all with an open probability of 0.31, and a ninth distinct channel with an open

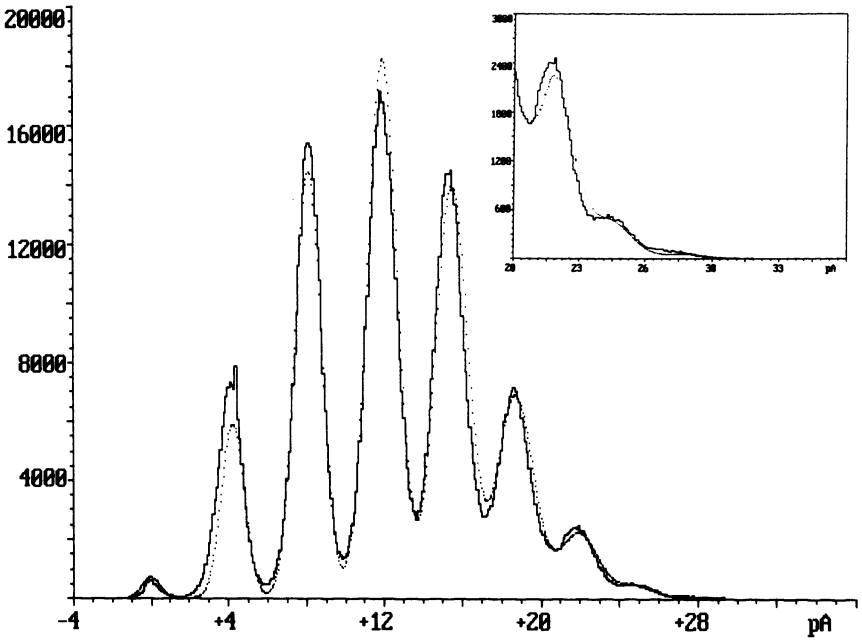


FIGURE 3 Amplitude histograms of the entire 8 min recording of a 94-pS channel at +45 mV. CsCl concentration was 135 mM in bath and pipette. The inset shows an enlargement of the smaller peaks. The dotted line in the large illustration is the fit made using Eq. 4 for independent channels, assuming two types of channels. Eight channels, all with an open probability of 0.31, and a ninth distinct channel, with an open probability of 0.87, are used. The variances used are $\sigma_b = 0.48$ pA and $\sigma_o = 0.33$ pA for the thermal and open channel noise, respectively. The currents for the different levels (see Eq. 7 of text) are $I_1 = 4.22$ pA, $I_2 = 8.09$ pA, $I_3 = 11.89$ pA, $I_4 = 15.46$ pA, $I_5 = 18.71$ pA, $I_6 = 21.9$ pA, $I_7 = 24.7$ pA, $I_8 = 28.2$ pA, and $I_9 = 31.5$ pA. The y-axis is the number of digitized points.

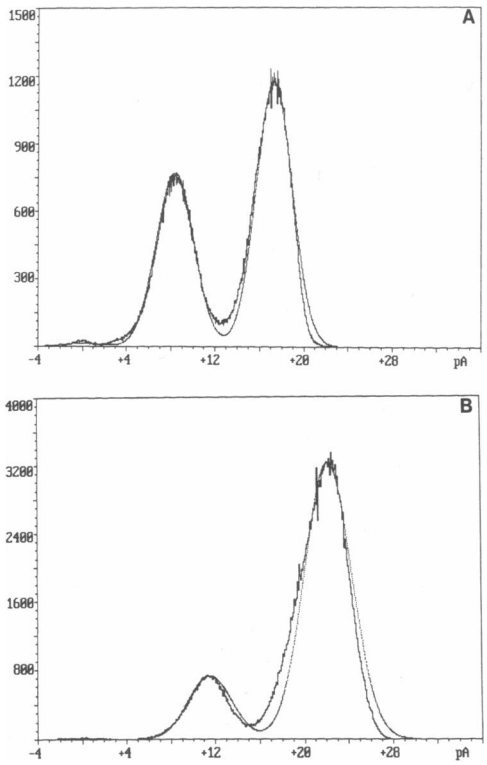


FIGURE 4 (*A*) An amplitude histogram where at least two channels were present in a patch. Both sides of the patch contained 170 mM CsCl saline. The holding potential was +60 mV; the unitary current at first open level was 8.40 and the second was 17.3 pA. The histogram required two different open probabilities (0.98 and 0.60) to be fit. (*B*) The bath solution was exchanged for one that contained 340 mM CsCl, and the unitary current levels were 11.5 and 22 pA. Again two different open probabilities (0.98 and 0.84) were required. The histogram peaks shifted proportionately when exposed to a saline that changed the equilbrium potentials for Cl and Cs. The *y*-axis is the number of digitized points.

probability of 0.87. The need for a second type of channel may also be seen on inspection of the histogram.

We demonstrate that, at least to a first approximation, the channels with differing open probabilities are "similar" in the sense defined in the introduction. An excised patch was first recorded from with identical solutions on both sides (Fig. 4 *A*). The amplitude histogram could not be fit by one probability alone. It required that there be one channel with an open probability of 0.98 and another of 0.60. The peak current at the first open level was 8.4 pA and at the second it was 17.3 pA. Substates are the presumed reason for the apparent variation in unitary current from level to level. The total duration analyzed was 2 min. The smooth line is the best fit with the two open probabilities. Fig. 4 *B* shows that the same patch after the bath solution (170 mM CsCl) was exchanged by perfusion with a 340-mM CsCl solution. This caused $E_{Cs}$ and $E_{Cl}$ to go from 0 to +17 and −17 mV, respectively. If there were two different channels within the patch, the unitary peak currents of the histogram would not remain equivalent. If, on the other hand, similar channels with the same conductance and selectivity but different open probabilities were the case, the prediction would be as it is displayed in Fig. 4 *B*. The unitary currents were 11.5 and 22 pA, and two open probabilities were required to fit the histogram (0.98 and 0.84), a condition similar to that of Fig. 4 *A*. The duration of the analyzed recording was 2 min. The important point of Fig. 4 is that, to a first approximation, the channels observed in the excised patch, though they have differing probabilities of opening, are "similar." The smooth curve of Fig. 4 *B* is the fit using the open probabilities already given with Eq. 7. Brink and Fan (1989) showed that the septal membrane gap junction–like channel was permeant to cations and anions. The illustration shown here is consistent with those results. Further, as in previous studies (Brink and Fan, 1989), both bath and pipette contained molecules capable of specifically blocking other channel types such as anion channels ($Zn^{++}$), $Ca^{2+}$ channels ($Ni^{++}$, $Co^{++}$), and K channels (Cs, TEA). The same precautions were implemented in the experiments demonstrated in this study.

Another example of independent channels with different open probabilities is shown in Fig. 5. The data illustrated are an analysis of 8 min of a recording (071890 in Tables 1 and 2) from a excised patch at a potential of +61 mV. A maximum of two channels was observed during the entire record. The probability of both channels being closed is 0.0039, the number of complete closures is 34, and the mean time of a closure is 58.4 ms. The right inset in Fig. 5 shows one of the 34 closures in the record. The parameter Δ from Eq. 4 is 105, implying the existence of two different channel types (different open probabilities). The histogram requires one channel with an open probability of 0.54 and another channel with an open probability of 0.99 to be fit adequately. Again, Table 1 demonstrates that the record is stable for this case using the variance criteria.

## Case 3: Cooperative channels

Recall that, for two channels, if Δ as determined by Eq. 4 is $<4$, the channels are not acting independently (see Eq. 10). Fig. 6 shows the histogram of a 2.3-min recording (080890 in Table 2) from an excised patch at a potential of +50 mV. The maximium number of channels observed was two, which we take to be the number of channels in the patch. The parameter Δ was 1.4, which violates the independence requirement ($\Delta \geq 4$, Eqs. 9 and 10). The best fit of the data for two independent

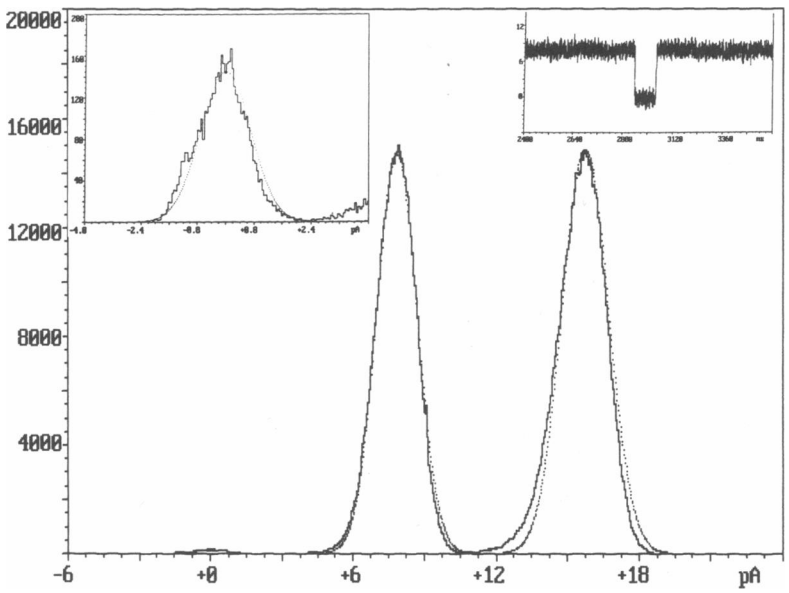


FIGURE 5 Amplitude histograms of an 8 min recording of a 130-pS channel at +61 mV. CsCl concentration was 170 mM in bath and pipette. The right inset shows one of the 34 closures in the record. The left inset shows an enlargement of the closed peak. The dotted line in the large illustration is the fit made using two different types of channels. One channel with an open probability of 0.54 and one channel with an open probability of 0.99 are used. The variances used are $\sigma_c$ = 0.7 pA and $\sigma_o$ = 0.48 pA for the thermal and open channel noise, respectively. The currents for the different levels (see Eq. 7 of text) are $I_1$ = 7.95 pA and $I_2$ = 15.75 pA. The y-axis is the number of digitized points.

channels is shown by the dotted line. In general, these channels range from 6 to 50 openings/minute per channel (Brink and Fan, 1989). In 2.3 min, only 500 events typically occur with two channels in the patch. We note that such violation of independence in a record cannot be explained away by mode shifting as detailed in the theory section, provided that the length of the record is sufficient. One scenario for this behavior could be that both channels have a high open probability for a certain time, and then "drop out" simultaneously for the remaining time. This simultaneous dropping out would be an example of cooperativity. Algebraically, it would invalidate the equality sign in Eq. 11 and thus may lead to violation of the independence criterion (Eq. 9). The record would also appear to be unstable according to the stability criterion; but, in the absence of a specific kinetic model for the channel, it is unclear whether the $5\sigma_p$ criterion presented in the stability section is sufficient to detect such nonstationarities. Recently, Dabrowski et. al. (1990) have presented sophisticated tests to examine the independence of channels under precisely these circumstances without knowledge of the kinetic model. We are currently implementing the algorithims in Dabrowski et al. (1990).

An issue is how often were the three cases observed in recordings found to be stable (criteria: variance). Table 2 displays the results of analysis of 20 data sets from 11 different excised patches. The table gives the number and the associated probabilities of channel types required to fit the amplitude histograms. Note that in six cases (30% of the total), one channel type was sufficient to give a good fit. Only one of the seven two-channel recordings exhibited cooperative behavior. 60% of the data analyzed required the use of two probabilities to fit the data.

A final issue is one referred to earlier as drop-out/drop-in. Two of the data sets shown in Table 2 demonstrate run-down or drop-out. 033089 started out with at least nine channels, and after some time only four channels were observable. Later in the experiment the number of channels increased to five, an example of drop-in. 033189 shows a similar drop-in from two to three channels.

## DISCUSSION

The gap-junctionlike channel in the earthworm septa shows evidence of being a heterogenous channel type, i.e., the channels may be similar but are not identical. We have demonstrated the existence of more than one channel type with respect to open probability, if the channels are independent. There is also a suggestion in some patches that the data cannot be fit by assuming independent channels. Nonindependent channels are also a possible explanation in cases where we have fit the

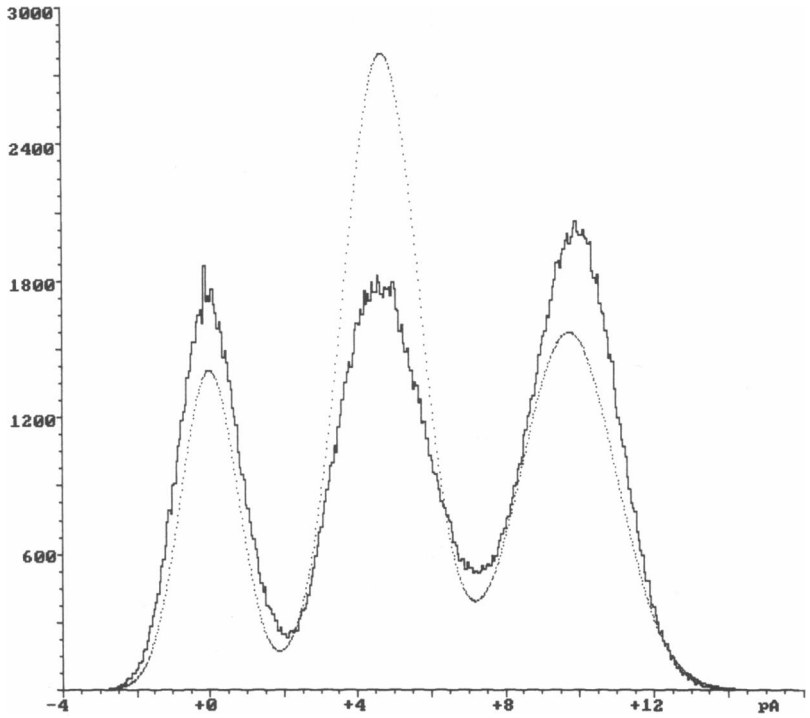


FIGURE 6 Amplitude histogram of a 2.3-min recording of a 93-pS channel at +50 mV. The dotted line is the fit made using Eq. 3 in the text for independent and identical channels. Eq. 8 of the text shows that the probabilities of the two channels required to fit the data are complex numbers. We have used two channels with an open probability of 0.43 to produce the fit; this is the real part of the complex number for the probability obtained by solving Eq. 8. This may be an example of cooperating channels in the sense of Eq. 10 of the text. The variances used were $\sigma_c = 0.64$ pA and $\sigma_o = 0.84$ pA for the thermal and open channel noise, respectively. The currents for the different levels (see Eq. 3 of text) are $I_1 = 4.64$ pA and $I_2 = 9.52$ pA. The solution on both sides of the membrane contained 135 mM of CsCl. The y-axis is the number of digitized points.

data assuming two open probabilities and independent channels.

If the channels we have observed in this study are derived from a population of independent and different channels, attractive structural explanations are possible, assuming the channel being studied is indeed a gap-junction channel. The connexin form is not known in the earthworm and all other invertebrates, but at least three vertebrate generic connexin subunit types (connexins Cx26, Cx32, and Cx43) (see Beyer et. al., 1987; Beyer, 1990) are known to be constituents of gap-junction channels. It is quite possible that one channel type is composed of Cx43 subunits alone, while another is composed entirely of Cx26 or 32 subunits. A further possibility is that some channels might be a mix of different subunits (43, 32, and 26 mixed) or even that one hemichannel is composed of subunits different from those of its apposed partner. For any of these and other cases, we can conceive of channels that are similar functionally (i.e., in selectivity and conductance) but different in terms of form (i.e., subunit composition).

If, on the other hand, we choose to interpret the data as due to identical and nonindependent channels, the morphological properties of gap junctions can still offer structural explanations. This is because—as also noted in the introduction—individual gap-junction channels tend to aggregate. In the case of the earthworm septa, and in many other systems as well, the gap-junction plaques usually contain tens or hundreds of channels. The channels themselves appear to be either in very close proximity to each other or in physical contact. Whether channel–channel connections, if they exist, are of a protein–protein or protein–lipid–protein form is not known at present. Such connections, whatever form they take, could be the explanation for the apparently non-identical channels needed to explain the data.

A final explanation is that all the channels are independent but "mode shifting" is a dominant aspect of channel function (Hess et al., 1984; McManus and Magleby, 1988). In this scenario, some channels can remain in a "mode" with a high open probability for an extended period of time. In some of the data sets analyzed here, we then find that the duration of such mode shifts is of the order of minutes. In a physiological time scale this is tantamount to saying that there are different channel types within the patch or at least

functionally dissimilar channels. Presumably, mode shifting reflects a change in state of the channel protein. Such a change could occur through the binding or unbinding of a ligand or through a change in the state of phosphorylation of the channel. The drop-in and drop-out phenomenon that we have observed suggests that some such factor that is beyond our control is affecting these channels.

If both independent and cooperative behavior are norms in the world of gap junctions, then multichannel recordings will be a necessary complement to recordings of single channels to elucidate the full spectrum of behavior of such channels. Analysis of such recordings may be of some consequence in the modeling of action potential propagation in heart and other tissue (Cole et al., 1988).

*Received for publication 19 February 1991 and in final form 9 September 1991.*

## REFERENCES


Abramowitz, M., and I. Stegun. 1970. Handbook of Mathematical Functions. Dover Publications Inc., New York. 1046 pp.

Beyer, E. C. 1990. Molecular cloning and developmental expression of two chick embryo gap junction proteins. *J. Biol. Chem.* 265:14439–14443.

Beyer, E. C., D. L. Paul, and D. A. Goodenough. 1987. Connexin43: A protein from rat heart homologous to a gap junction protein from liver. *J. Cell Biol.* 105:2621–2629.

Brink, P. R., and S.-F. Fan. 1989. Patch clamp recordings from membranes which contain gap junction channels. *Biophys. J.* 56:579–593.

Cole, W. C., J. B. Picone, and N. Sperelakis. 1988. Gap junction uncoupling and discontinuous propagation in the heart. A comparison of experimental data with computer simulations. *Biophys. J.* 53:809–818.

Colquhoun, D., and A. G. Hawkes. 1981. On the stochastic properties of single ion channels. *Proc. R. Soc. Lond. B Biol. Sci.* 211:205–235.

Colquhoun, D., and F. J. Sigworth. 1983. Fitting and statistical analysis of single-channel records. *In* Single-Channel Recording. B. Sakmann and E. Neher, editors. Plenum Press, New York. 191–263.

Cox, D. R., and H. D. Miller. 1965. The Theory of Stochastic Processes. Chapman and Hall Ltd., London. 398 pp.

Dabrowski, A. R., McDonald, D. and Rösler, U. 1990. Renewal theory property of ion channels. *Annals of Statistics.* 18:1091–1115.

Fredkin, D. R., M. Montal, and J. A. Rice. 1985. Identification of aggregated Markovian models: application to the nicotinic acetylcholine receptor. *In* Proceedings of the Berkeley Conference in Honor of Jerzy Neyman and Jack Kiefer. L. M. Le Cam and R. A. Ohlsen, editors. Wadsworth Publishing Co., Belmont, CA. 269–289.

Goodenough, D. 1975. The structure and permeability of isolated hepatocyte gap junctions. *Cold Spring Harbor Symp. Quant. Biol.* 40:37–44.

Hess, P., J. B. Lansman, and R. W. Tsien. 1984. Different modes of Ca channel gating behavior favoured by dihydropyridine Ca agonists and antagonists. *Nature (Lond.).* 311:538–544.

Horn, R., and K. Lange. 1983. Estimating kinetic constants from single channel data. *Biophys. J.* 43:207–223.

Kensler, R. W., P. R. Brink, and M. M. Dewey. 1977. Glial cells in the earthworm ventral cord make an A-type nexus. *Am J. Anat.* 149:605–611.

Kensler, R. W., P. R. Brink, and M. M. Dewey. 1979. The septum of the lateral axon of the earthworm: a thin section and freeze fracture study. *J. Neurocytol.* 8:565–590.

Korn, H., A. Triller, A. Mallet, and D. S. Faber. 1981. Fluctuating responses at a central synapse: *n* of binomial fit predicts number of stained pre synaptic boutons. *Science (Wash. DC).* 213:898–900.

Läuger, P. 1983. Conformational transitions of ionic channels. *In* Single-Channel Recording. B. Sakmann and E. Neher, editors. Plenum Press, New York. 177–189.

McManus, O. B., and K. L. Magleby. 1988. Kinetic states and modes of single large-conductance calcium-activated potassium channels in cultured rat skeletal muscle. *J. Physiol (Lond.).* 402:74–120.

Sachs, F., J. Neil, and N. Barkakati. 1982. The automated analysis of data from single ionic channels. *Pflügers Arch.* 395:331–340.

Sigworth, F. J. 1985. Open channel noise. I. Noise in acetylcholine receptor currents suggests conformational fluctuations. *Biophys J.* 47:709–720.

Stevens. C. F. 1972. Inferences about membrane properties from electrical noise measurements. *Biophys J.* 12:1028–1047.

Tuttle, R., S. Masuko, and Y. Nakajima. 1986. Freeze-fracture studies of the large myelinated club ending synapse of the goldfish Mauthner cell: special reference to the quantitative analysis of gap junctions. *J. Comp. Neurol.* 246:202–211.